

11 **Abstract**

12 Understanding biological processes, such as growth, is crucial to development management and
13 sustainability plans for bivalve populations. von Bertalanffy and Gompertz models have been commonly
14 used to fit bivalve growth. These models assume that individual growth is only determined by size,
15 overlooking the effects of environmental and intrinsic conditions on growth patterns. The comparison
16 between classical models and nonparametric GAM (generalized additive models) fits conducted in this
17 work shows that the latter provide a more realistic approach of mussel growth measured in terms of shell
18 length, and dry weight of hard and soft tissues. GAM fits detected a reduction in growth during the cold
19 season, under unfavourable nutritional conditions. These fits also captured the decoupling between hard
20 and soft tissue growth, widely addressed in the literature but not incorporated in growth models. In
21 addition a GAM fit of condition index allowed us to explain annual changes in resources allocation,
22 identifying the asymptotic growth of shell and the effects of the reproductive cycle on soft tissue
23 fluctuations.

24 **Keywords:** condition index, GAM, Gompertz, shell, soft tissue, von Bertalanffy

25 **Introduction**

26 Mussels are dominant organisms on many rocky shores worldwide, where they play an important
27 ecological role as habitat or prey for a multitude of organisms (Rilov et al., 2008), and in the pelagic-
28 benthic coupling (Alonso-Pérez et al., 2010; Dame, 1993; Zúñiga et al., 2014). In addition, mussel
29 aquaculture is a sustainable food production system with important commercial (Díaz et al., 2014;
30 Labarta et al., 2004) and environmental value, since mussel farming has been proposed as a tool to
31 mitigation of eutrophic coastal areas (Lindahl et al., 2005). The growing importance of aquaculture in
32 food production along the past decades has resulted on an increasing demand for management and
33 sustainability plans (Bergström et al., 2015). Understanding how biological processes, such as
34 reproduction or growth, respond to environmental changes is crucial to improve management strategies.

35 The most commonly applied growth models are those proposed by Gompertz (1825) and von
36 Bertalanffy (1938). The latter is thought to be a better describer of growth in fish and bivalves (Gosling,
37 2003). These models focus on characterizing the mean growth pattern of a given species along its
38 lifespan. For this purpose both von Bertalanffy and Gompertz models assume that individual growth is
39 asymptotic and that the growth rate is only determined by size. However development of management
40 and sustainability plans requires understanding the growth dynamics and seeks for models able to detect
41 seasonal or short-term changes in bivalve growth.

42 It is well known that bivalve growth is driven by intrinsic physiological processes and
43 influenced by environmental conditions. During the past decades several works have highlighted the
44 effect of factors such as physiological dynamics, ecological memory, and environmental conditions on
45 bivalve growth (Babarro et al., 2000; Blicher et al., 2010; Borrero and Hilbish, 1988; Hilbish, 1986;
46 Kautsky, 1982; Lewis and Cerrato, 1997; Mallet et al., 1987; Okumuş and Stirling, 1994; Pérez-Camacho
47 et al., 2014, 1995). Two different strategies have been adopted to account for these effects. Some works
48 have fitted von Bertalanffy (Bagur et al., 2013; Connor and Robles, 2015; Nedoncelle et al., 2013;
49 Ozernyuk and Zotin, 2006) and Gompertz (Cubillo et al., 2012; Irisarri et al., 2015; Peteiro et al., 2008,
50 2006) models to populations growing under different conditions and compared the fitted parameters to
51 test whether the factors under study affected bivalve growth. Other works have developed extended von
52 Bertalanffy models incorporating the effects of food availability (Marambio et al., 2012) or maturity
53 status (Ohnishi et al., 2012) on bivalve growth.

54 An important feature of bivalve growth, which deserves special attention to schedule aquaculture
55 production, is the decoupling between hard and soft tissue (Blicher et al., 2010; Borrero and Hilbish,
56 1988; Hilbish, 1986; Lewis and Cerrato, 1997; Witbaard et al., 2015). This decoupling can be attributed
57 to a mismatch between the favourable conditions to shell growth and those leading to increases of soft
58 tissue (Borrero and Hilbish, 1988), and to seasonal changes in the allocation of resources between growth
59 and reproduction (Peterson and Fegley, 1986). Despite these evidences, changes in shell length and soft
60 tissue have been wrongly used as equivalent measures of growth and consequently classical and new
61 parametric growth models have overlooked this uncoupling. For instance the extended von Bertalanffy
62 model introduced by Ohnishi and Akamine (2006) to incorporate hard and soft tissue growth patterns
63 assumes an allometric relationship between hard and soft tissue growth rates, in contrast with the
64 observed uncoupling.

65 The common practice in fish and bivalve growth modelling is to select a model, usually von
66 Bertalanffy or Gompertz, and fit this model to the data. This procedure can lead to biased estimators, and
67 consequently wrong decisions, when the observed data are inconsistent with the selected model. Recent
68 studies (Katsanevakis and Maravelias, 2008; Rabaoui et al., 2007; Rogers-Bennett, 2003) have pointed
69 out this problem and proposed the Akaike Information Criterion (AIC) as goodness-of-fit measure to
70 select the best growth model among a set of candidates. Once again this procedure relies on the subjective
71 selection of some candidate models leading to unrealistic estimates if none of them is consistent with the
72 real data.

73 Recent works have applied semiparametric approaches, such as generalized additive models
74 (GAM, Hastie and Tibshirani, 1990) to include environmental and endogenous variables in fish growth
75 curves (Ligas et al., 2015; Olsen et al., 2006; Smith et al., 2005). For bivalves, some authors have
76 computed instantaneous growth rates as the ratio between shell length increase and time between
77 sequential samplings and applied GAM to fit the corresponding temporal pattern (Katsanevakis, 2007;
78 Witbaard et al., 2015). To our knowledge any comparison between the performance of classical and
79 semiparametric approaches, which would check the goodness-of-fit of the former, has not been conducted
80 up to date.

81 To address the management of both wild and cultured bivalve populations at ecosystem level we
82 need procedures able to detect short-term or seasonal changes in the growth pattern of bivalves. This

83 work is a first attempt to test whether the commonly used von Bertalanffy and Gompertz provide accurate
84 fits for the growth patterns of hard and soft tissues in the mussel *Mytilus galloprovincialis* (Lamarck,
85 1819) or more flexible procedures are required. For this purpose, we have considered our dataset used
86 previously in Babarro et al. (2003), which analyzed mussel growth in suspended culture using the
87 classical models. We tested the goodness-of-fit of the von Bertalanffy and Gompertz models through
88 comparison with GAM fits. Instantaneous growth rates were also estimated as the first derivatives of the
89 fitted models, in contrast with previous works that estimated instantaneous growth rates as the average
90 change in size between samplings. Finally we tested whether GAM models can detect differences
91 between the growth patterns of hard and soft tissues.

92 **Materials and methods**

93 *Experimental design*

94 Seed of *Mytilus galloprovincialis* with a mean shell length of 21.2 mm (sd =8.5) was gathered
95 from collector ropes on a raft located in the mid-to-outer area of the Ría de Arousa (Galicia, NW Iberian
96 Coast, see Figure A.1 in appendix A), and were socked on culture ropes deployed in an adjacent
97 commercial raft in January 1998. Culture ropes were kept in the water up to July 1999 (526 days)
98 covering both pre-fattening, up to November 1998, and fattening, from November 1998 to harvest in July
99 1999, phases of mussel culture (see details in Babarro et al. (2003)).

100 *Sampling procedure*

101 Sequential samplings were conducted on 28 January (seeding), 11 March, 6 May, 3 June, 1 July,
102 24 September and 11 November during 1998; and on 24 February, 28 April, 26 May and 7 July (harvest)
103 during 1999. Duplicated samples of 200-300 individuals were taken from adjacent ropes in each sampling
104 date. Individual mussel length (L, mm) was measured to the nearest 1 mm using callipers to obtain the
105 mean shell length of each sample. Subsamples of 5-15 mussels each from 5-6 length classes covering the
106 whole size range were used to determine total (TDW, g), shell (DWs, g) and tissue dry weight (DWt, g)
107 by dissection and after drying at 100° C until constant weight. Condition index was calculated as the ratio
108 between tissue and shell dry weights, $CI=DWt/DWs$ (Lucas and Beninger, 1985).

109 *Data analysis*

110 *Classical growth models*

111 Specific von Bertalanffy (vB) and Gompertz (G) models were used to fit growth curves in terms
 112 of shell length (mm), total, shell and tissue weight (g). The von Bertalanffy and Gompertz models for
 113 shell length are defined as follows:

114
$$vB : L_t = L_\infty \left(1 - e^{-k(t-t_0)} \right) \quad (1)$$

115
$$G : L_t = L_\infty \exp\left(-e^{-k(t-t^*)}\right) \quad (2)$$

116 where L_∞ (mm) represents the asymptotic length, L_t (mm) is the shell length at time t (months), k is the
 117 growth parameter indicating the speed at which asymptotic growth is attained, t_0 (1) represents the
 118 theoretical time at which length is 0, and t^* (2) denotes the time of growth inflexion. The same models
 119 were used to fit growth curves in terms of weight.

120 The first derivatives of the models under comparison were computed to estimate growth rates
 121 along the culture period. For the von Bertalanffy and Gompertz model we used the expressions:

122
$$vB : \frac{\partial L}{\partial t} = kL_\infty e^{-k(t-t_0)} \quad (3)$$

123
$$G : \frac{\partial L}{\partial t} = ke^{-k(t-t_0)} L_\infty \exp\left(-e^{-k(t-t_0)}\right) = kL_t e^{-k(t-t_0)} \quad (4)$$

124 *GAM fit of growth curves*

125 Despite von Bertalanffy (eq. 1) and Gompertz (eq. 3) models have been widely used to estimate
 126 mussel growth in terms of shell length (mm) and dry weight (g), they can be very restrictive and lead to
 127 biased estimations and consequently incorrect conclusion when the data do not support the relationships
 128 imposed by these models. Nonparametric regression techniques provide an approach to growth curves
 129 without specifying in advance any function for the effect of time on size. Therefore mussel growth can be
 130 expressed as follows

131
$$Y = E[Y|t] + e = m(t) + e \quad (5)$$

132

133 where Y is the size measure, m is an unknown smooth function and e is the error term. In this work, m
 134 was fitted using regression splines, i.e. we applied a generalized additive model (GAM, Hastie &
 135 Tibshirani, 1990; Wood, 2006), which can be defined as follows:

$$136 \quad E[Y|t] = H(\alpha + f(t)) \quad (6)$$

137 where α is the intercept, f_j is an unknown smooth function, which in this case was fitted by thin plate
 138 regression splines, and H is a fixed, known, monotone link function, selected according to the distribution
 139 of the response variable, Y . In this work we fitted GAM with Gaussian family and “identity” link function
 140 for shell length and dry weight, which were normally distributed (Shapiro test, p-value > 0.05). A GAM
 141 (1) with Gamma family and logarithmic link was applied to fit the temporal pattern of condition index.
 142 We also computed the first derivative of the GAM fits to obtain instantaneous growth rates.

143 *Testing the goodness-of-fit of the classical growth models*

144 Graphical comparison of the growth curves provided by the classical and GAM fits can be used
 145 to check the accuracy of von Bertalanffy and Gompertz models. Classical models are correct when the
 146 corresponding growth curves lay within the 95% confidence interval of the GAM growth curves.
 147 Nevertheless we also conducted a formal goodness-of-fit test for this purpose.

148 We applied a Generalized likelihood ratio (GLR) test (Fan and Jiang, 2007) to check the
 149 goodness-of-fit of the classical von Bertalanffy and Gompertz models, that is, to test whether any of these
 150 models provides a correct specification of the growth curves. Thus, considering the general model in
 151 equation (3), we test the null hypothesis $H_0: m(\text{time}) = m_0(\text{time})$, where m_0 is given by expression (1) for
 152 von Bertalanffy and expression (2) for Gompertz, respectively, versus the general alternative hypothesis
 153 H_1 where m is an unknown smooth function estimated by GAM. Let $\{t_i, Y_i\}_{i=1}^n$ be the observed data, the
 154 likelihood ratio test is

$$155 \quad T = \frac{n}{2} \log \frac{RSS0}{RSS1} = \frac{n}{2} \log \frac{\sum_{i=1}^n (Y_i - m_0(t_i))^2}{n^{-1} \sum_{i=1}^n (Y_i - m(t_i))^2} \quad (7)$$

156 where $RSS0$ and $RSS1$ are the maximum likelihood estimators for the error variance under H_0 and H_1 ,
 157 respectively. For a fixed significance level α , we reject the null hypothesis when $T > T^{1-\alpha}$, where $T^{1-\alpha}$ is
 158 the $100(1-\alpha)$ -percentile of T under H_0 . As asymptotic theory for nonparametric tests is not closed yet, we
 159 can apply resampling methods such as bootstrap (Efron and Tibshirani, 1994) to calibrate the test. Wild
 160 bootstrap (Hardle and Mammen, 1993) was used in this case to generate the resamples. Thus the
 161 empirical p-value of the test is the proportion of simulated T values larger than that obtained for the
 162 observed data. The algorithm performed to conduct this goodness-of-fit test is detailed in Appendix A.2.

163 *Comparison of shell and soft tissues growth patterns*

164 In order to test whether hard and soft tissue growths are coupled, we used a GAM fit with
 165 interaction factor (type of tissue) by curve (time) defined as follows:

$$166 \quad E[Y|t, Z] = H \left(\alpha_j I(Z = Z_j) + \sum_{j=1}^2 f_j(t) I(Z = Z_j) \right) \quad (8)$$

167 where, $j=1,2$ identifies the group defined by hard (shell) and soft tissue, α_j , is the intercept for the j th type
 168 of tissue. And f_j is the smooth function that describes the effect of time on the response for the j th type of
 169 tissue. As well as in model (5) we used Gaussian family with “identity” link function (H).

170 We used the shrinkage variable selection procedure proposed by Marra and Wood (2011) to test
 171 whether the effect of time on each response variable depends on type of tissue, i.e. to select between
 172 model (8) and the model without interactions:

$$173 \quad E[Y|time, Z] = H \left(\alpha_j I(Z = Z_j) + f(time) \right) \quad (9)$$

174 Once model selection was conducted, normality and independence of residuals were tested by
 175 the Shapiro-Wilk and Ljung–Box tests, respectively. In addition to the growth curves, we fitted their first
 176 derivatives in order to estimate growth rates along the culture period.

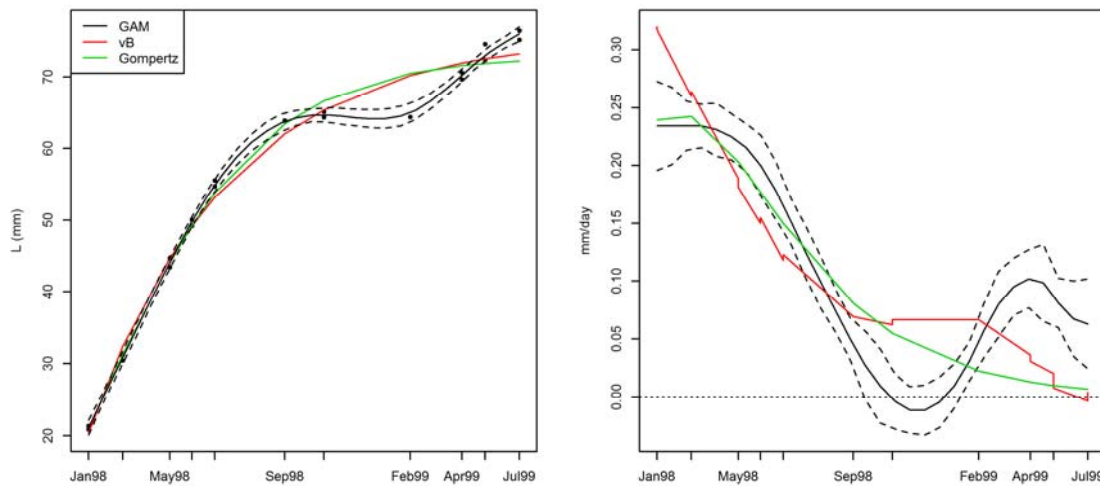
177 *Software*

178 Data analysis was performed with the statistical software R.3.1.3 (R Development Core Team,
 179 2015). In particular, the `nls` function in the `stats` package was used to fit Gompertz and von Bertalanffy

180 models by nonlinear least squares (Bates and Watts, 1988), and the *mgcv* package (Wood, 2006) was used
181 to fit the GAM models.

182 Results

183 Figure 1 shows that the GAM (eq. 5) and classical growth models -von Bertalanffy (eq. 1) and
184 Gompertz (eq. 2) provide similar growth curves up to September 1998. Although the GLR tests accept the
185 goodness-of-fit of both classical models (p -value > 0.1 , Table B1 in Appendix B), we observe differences
186 between models from autumn onwards when the GAM detects stagnation in shell length growth, which
187 was not identified by the classical models. In Appendix B (Figure B1, Table B1) we report the result for
188 growth curves in terms of weight. The GLR tests (Table B1) point out the lack of fit of the classical
189 growth models, mainly for tissue dry weight. In view of these results GAM fits shall be used to estimate
190 the different growth curves considered along this work.



191

192 **Figure 1:** Comparison of growth models. Observed shell lengths (points), GAM (black), von Bertalanffy (vB, red),
193 Gompertz (G, green) fits of growth curves (left) and their first derivative (right). Fitted values (solid line) and 95%
194 confidence intervals (dashed lines) for GAM fit.

195 The model selection conducted to test for differences between the growth patterns of shell and
196 soft tissue detected a significant effect of type of tissues on the intercept (p -value ≈ 0) and smooth terms
197 of the growth curves in terms of dry weight (p -value ≈ 0), indicating a mismatch between the growth of
198 hard and soft tissues. Indeed the AIC for model (8), which assumed different growth patterns for hard and
199 soft tissue (AIC = 16.33) was smaller than that obtained overlooking the differences between tissues

200 (model (9), AIC=152.29). Therefore, model (8) was used to estimate the growth patterns of shell (DWs)
 201 and tissue (DWt) dry weight.

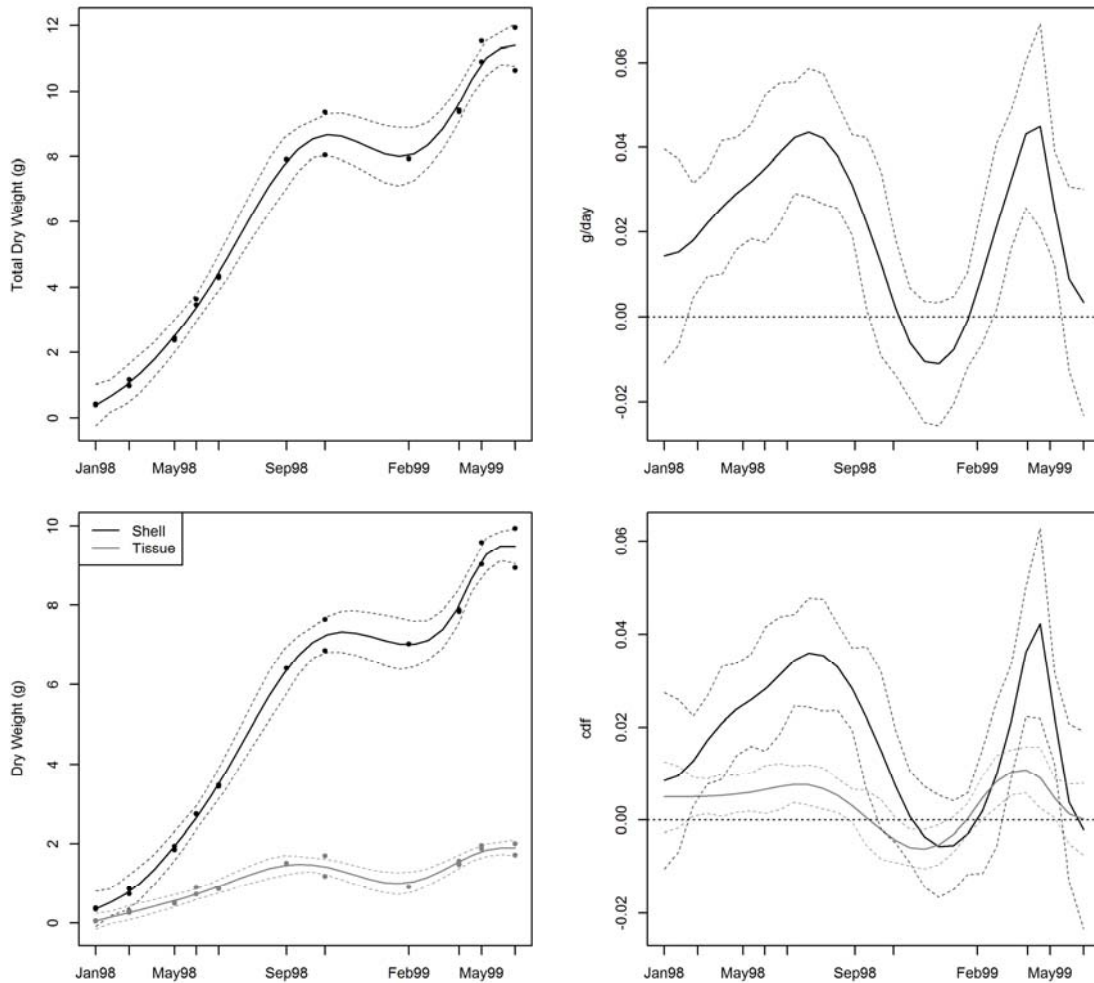
202 A summary of the fitted models, goodness-of-fit measures and tests conducted for model
 203 checking is shown in Table 1. Shell length increased up to October; stagnated during autumn-winter, and
 204 increased again from February onwards, but at a lower rate than during the first spring (Figure 1). As
 205 observed for shell length (Figure 1), total (Figure 2, top) and shell dry weight (Figure 2, bottom, black
 206 lines) stopped growing from October to March. Nevertheless, soft tissue (Figure 2, bottom, grey lines)
 207 increased up to September, decreased from November to February and increased again from March
 208 onwards.

209 **Table 1:** GAM fits of mussel growth in terms of shell length (L, mm) total dry weight (TDW, g), shell dry weight
 210 (DWs, g), tissue dry weight (DWt, g), and condition index (CI = DWt/DWs). Normality of residuals was tested
 211 through the Shapiro–Wilk (SW) while independence of residuals was checked through the Ljung–Box (LB) tests.

	Parametric coefficients					Goodness of fit		Residuals	
	Estimate	Std. Error	t value	Pr(> t)	Adj R ²	%Dev Exp	SW	LB	
L (mm)	Intercept	54.903	0.169	325.5	<2e-16 ***	0.998	99.90%	0.0969	0.4327
	Smoth terms								
		edf	Ref.df	F	p-value				
	s(time)	6.673	9	1194	<2e-16 ***				
TDW (g)	Parametric coefficients					Goodness of fit		Residuals	
	Estimate	Std. Error	t value	Pr(> t)	Adj R ²	%Dev Exp	SW	LB	
	Intercept	6.027	0.103	58.62	8.7e-16 ***	0.997	99.20%	0.1462	0.1760
	Smoth terms								
	edf	Ref.df	F	p-value					
	s(time)	7.327	9	162.2	<2e-16 ***				
DWs vs DWt (g)	Parametric coefficients					Goodness of fit		Residuals	
	Estimate	Std. Error	t value	Pr(> t)	Adj R ²	%Dev Exp	SW	LB	
	(Intercept)	4.981	0.054	91.77	<2e-16 ***	0.994	99.60%	0.0495	0.0179
	Tissue	-3.936	0.077	-51.27	<2e-16 ***				
	Smoth terms								
	edf	Ref.df	F	p-value					
	s(time):Shell	8.594	9	417.4	<2e-16 ***				
	s(time):Tissue	4.872	9	13.98	2.5e-14 ***				
CI	Parametric coefficients					Goodness of fit		Residuals	
	Estimate	Std. Error	t value	Pr(> t)	Adj R ²	%Dev Exp	SW	LB	
	Intercept	-1.525	0.026	-59.53	3.2e-15 ***	0.803	91.90%	0.5895	0.2529
	Smoth terms								
	edf	Ref.df	F	p-value					
	s(time)	7.936	8.684	14.02	1.6e-06 ***				

212 (***) p-value < 0.001, (**) p-value < 0.01, (*) p-value < 0.05, (.) p-value < 0.1.

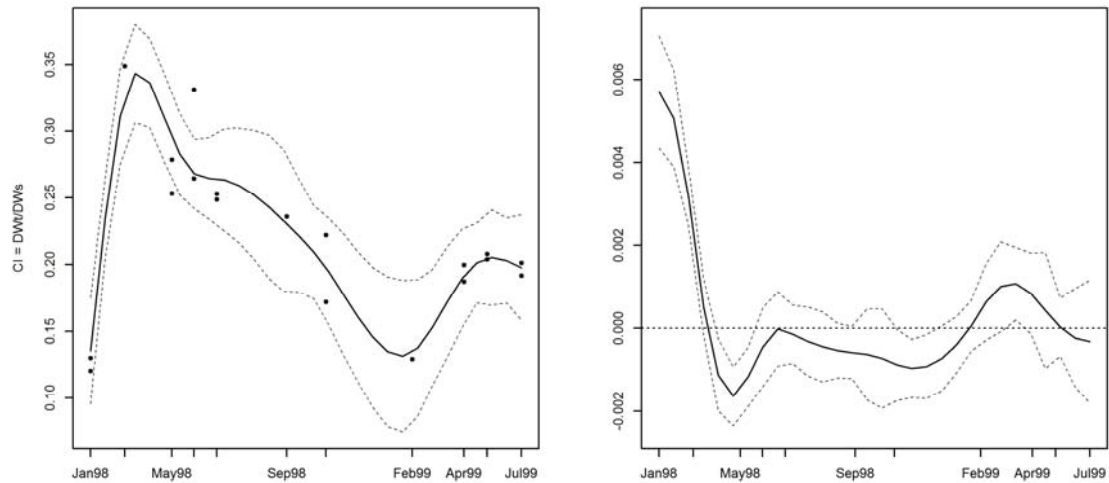
213



214

215 **Figure 2:** Mussel growth. Top: total dry weight (TDW, top). Bottom: shell (black) and tissue dry weight (grey).
 216 Observed values (points), and GAM fits of growth curves (left) and their first derivative (right). Fitted values (solid
 217 line) and 95% confidence intervals (dashed lines).

218 The differences between hard and soft tissue growth curves and the significant effect of time on
 219 the condition index (Table 1) indicate a temporal mismatch between the investment of mussels on shell
 220 and soft tissue. The decrease in CI during the first spring and winter (Figure 3) reflects two different
 221 situations: during spring both tissue and shell grew, but the latter grew at a higher rate; while the decrease
 222 in winter is caused by soft tissue losses (Figure 2, bottom). We also observe opposite behaviours between
 223 the first and second spring, as the latter reported an increase in the condition index (Figure 3), i.e. higher
 224 growth rates in soft tissue than in shell.



225

226 **Figure 3:** Condition index ($CI=DW_t/DW_s$). Observed values (points), and GAM fit of the temporal pattern of mussel
 227 CI (left) and its first derivative (right). Fitted values (solid line) and 95% confidence intervals (dashed lines).

228 **Discussion**

229 The important ecological and commercial role of bivalve aquaculture have motivated an
 230 increasing demand for management and sustainability plans (Bergström et al., 2015). Modelling
 231 individual growth is a key factor to understand the dynamics of these species and, consequently in the
 232 development of management and sustainability plans for aquaculture. Up to date, the majority of works
 233 have focused on spatial planning through the comparison of bivalve growth patterns at different locations
 234 (Bergström et al., 2015; Brigolin et al., 2009; Pérez-Camacho et al., 2014, 1995). Short term variability
 235 on bivalve growth in response to changes on the environmental conditions, which is crucial for site
 236 specific management plans, have received less attention.

237 Bivalve growth has been modelled by the classical von Bertalanffy and Gompertz models,
 238 which aim to estimate the mean growth along the individual lifespan and assume that growth is only
 239 determined by size. However a proper understanding of the growth dynamics requires detecting changes
 240 in the growth patterns along the culture period, as well as differences between hard and soft tissue growth.
 241 For this reason this work tests whether the classical growth models provide realistic fits of bivalve growth
 242 or more flexible techniques, such as GAM, are required

243 Although the small sample size ($n = 20$) can limit the power of the goodness-of-fit test, we have
 244 confirmed that von Bertalanffy and Gompertz models miss-specify mussel growth in terms of dry weight.

245 The GAM fit detected temporal variability in mussel growth, extensively described (Borrero and Hilbish,
246 1988; Gangnery et al., 2004; Hilbish, 1986; Kautsky, 1982; Lewis and Cerrato, 1997; Pernet et al., 2012;
247 Urrutia et al., 1999; Witbaard et al., 2015). The large amount of endogenous and exogenous variables
248 involved in a complex process such as bivalve growth, which hampers the development of accurate
249 parametric models for age-size relationships, and the goodness-of-fit of GAMs, which do not need to
250 assume any restrictive relationship between the response and the explanatory variables, support the use of
251 the latter to fit bivalve growth. The first order derivatives of the fitted growth curves provide accurate
252 estimates of the instantaneous growth rates, which up to date have been obtained as the ratio between size
253 increases and time between samplings (Katsanevakis, 2007; Witbaard et al., 2015), GAM fits also
254 detected a decoupling between hard and soft tissues, widely addressed in the literature (Blicher et al.,
255 2010; Borrero and Hilbish, 1988; Hilbish, 1986; Lewis and Cerrato, 1997; Witbaard et al., 2015) but not
256 incorporated to growth models.

257 The temporal variability on mussel growth detected by the GAM fits is in agreement with
258 important features such as the effect of the environmental conditions and the reproductive cycle on
259 bivalve growth, which have been described along several decades. The fitted growth curves and rates in
260 terms of shell length and shell weight reflect the common pattern at temperate latitudes, where shell
261 growth from spring to early autumn is favoured by optimal nutritional conditions and increasing
262 temperatures, in contrast with the low food availability in colder months (Kautsky, 1982; Loo and
263 Rosenberg, 1983; Mallet et al., 1987). Soft tissue losses during winter can be attributed to an early
264 spawning event. *Mytilus* species are thought to synchronize their reproductive cycle with favourable
265 environmental conditions (Edwards and Richardson, 2004; Newell et al., 1982; Philippart et al., 2012). In
266 coastal upwelling systems spawning of many invertebrate and fish species occurs during the upwelling
267 season (Otero et al., 2009; Snodden and Roberts, 1997; Suárez et al., 2005), which in the Galician Rías
268 extends between spring and autumn (Torres et al., 2003; Wooster et al., 1976).

269 The temporal pattern of the condition index suggest a higher investment in shell up to summer
270 followed by a period of isometric growth up to mid-autumn, i.e. the end of the upwelling season. In
271 agreement with these findings, Hilbish (1986) argued that in *Mytilus edulis* shell growth preceded soft
272 tissue growth. The decrease in CI during winter reflects soft tissue losses, which may be attributed to
273 energy investment on gametogenesis coupled with unfavourable nutritional and environmental conditions

274 (Witbaard et al., 2015) and the subsequent spawning event in late winter. The increase in CI during the
275 second spring indicates a higher investment on tissue than on shell, in contrast with the first spring. This
276 interannual shift may be attributed to the progressive reduction in shell growth as asymptotic size is
277 approached, and the post-spawning recovery of soft tissue. Accordingly, Peterson and Fegley (1986)
278 found that shell growth in juvenile clams was much higher than in adult clams. These results are in
279 agreement with the different hard and soft tissue growth patterns of bivalves. While shell growth is
280 asymptotic (Sebens, 1987), soft tissue of adult mussels undergo substantial annual changes mainly driven
281 by their reproductive cycle (Peterson and Fegley, 1986).

282 The decoupling between shell and soft tissues points out the need for testing whether mussels
283 fulfil the allometric length-weight relationship, widely used to describe relative bivalve growth (Cubillo
284 et al., 2012; Irisarri et al., 2015; Peteiro et al., 2008, 2006, Rabaoui et al., 2011, 2007). In this line Sestelo
285 and Roca-Pardinas (2011) and Martínez-Silva et al. (2014) show that nonparametric regression provides
286 a better fit for the relative growth of barnacles and sea urchins, which condition index also exhibit
287 seasonal variation, than allometric models.

288 The productivity of mussel farming, depend on individual size and meat yield, defined as the
289 ratio between meat and total fresh weight, since market prices are based on these parameters (Fuentes-
290 Santos et al., 2015; Pérez-Camacho et al., 2013). More exhaustive sampling procedures than those
291 required by the classical models, and the flexibility of nonparametric approaches, such as GAM, shall
292 capture short term variability of bivalve growth and meat yield. These approaches shall contribute to the
293 development of site specific management strategies through a proper schedule of seeding and harvesting.
294



297
 298 **Figure A 1:** Mussel culture polygons in the Ría de Arousa (Galicia, NW Spain). A: raft where the experimental
 299 culture was conducted. B: raft where mussel seed was collected.

300 *A.2 Details of the goodness-of- fit test.*

301 We applied a Generalized likelihood ratio test (Fan and Jiang, 2007) to check the goodness-of-fit of the
 302 classical von Bertalanffy and Gompertz models, that is, to test whether any of these models provides a
 303 correct specification of the growth curves. Thus, considering the general model in equation (3), we test
 304 the null hypothesis $H_0: m(t) = m_0(t)$, where m_0 is given by expression (1) for von Bertalanffy and
 305 expression (1) for Gompertz, respectively, versus the general alternative hypothesis H_1 where m is an
 306 unknown smooth function estimated by GAM. Let $\{t_i, Y_i\}_{i=1}^n$ the observed data, the likelihood ratio test
 307 is

308
$$T = \frac{n}{2} \log \frac{RSS0}{RSS1} = \frac{n}{2} \log \frac{\sum_{i=1}^n (Y_i - m_0(t_i))^2}{n^{-1} \sum_{i=1}^n (Y_i - m(t_i))^2} \quad (10)$$

309 where $RSS0$ and $RSS1$ are the maximum likelihood estimators for the error variance under H_0 and H_1 ,
 310 respectively. For a fixed significance level α , we reject the null hypothesis when $T > T^{1-\alpha}$, where $T^{1-\alpha}$ is
 311 the $100(1-\alpha)$ -percentile of the T under H_0 . As asymptotic theory for nonparametric tests is not closed yet,
 312 we can apply resampling methods such as bootstrap (Efron and Tibshirani, 1994) to calibrate the test.
 313 Wild bootstrap (Hardle and Mammen, 1993) was used in this case to generate the resamples. Thus, we
 314 applied the following algorithm to test the goodness-of-fit of the classical growth model.

- 315 1. Obtain the null, $m_0(t)$, and alternative, $m(t)$, regression functions for the sample data $\{t_i, Y_i\}_{i=1}^n$
 316 and compute the test statistic T_{obs} as defined in expression (7).
- 317 2. For $b = 1, \dots, B$ ($B = 10000$ in this work)
- 318 2.1. generate bootstrap resamples $\{t_i, Y_i^*\}_{i=1}^n$, with $Y_i^* = m_0(t_i) + e_i^*$ being

$$319 \quad e_i^* = \begin{cases} \frac{(1-\sqrt{5})e_i}{2} & \text{with probability } p = \frac{5+\sqrt{5}}{10} \\ \frac{(1+\sqrt{5})e_i}{2} & \text{with probability } p = \frac{5-\sqrt{5}}{10} \end{cases}$$

320 where $e_i = Y_i - m_0(t_i)$ are the errors of the parametric model in H_0 .

- 321 2.2. Given $\{t_i, Y_i^*\}_{i=1}^n$, compute T^{*b} as in step 1.
- 322 3. The empirical p-value of the test is the proportion of simulated T-statistics larger than that
 323 obtained for the observed data.

324

325 **Appendix B: Supplementary data for the Results Section**

326 This Appendix provides the parameters and the p-values of the likelihood ratio tests for the fitted von
 327 Bertalanffy and Gompertz models (Table B1). Figure B1 provides graphical comparison between
 328 classical and GAM fits of mussel growth in terms of total, shell and soft tissue weight .

329 **Table B1:** Parameters of the von Bertalanffy and Gompertz fits for shell length (L), total (TDW), shell (DWs), and
 330 tissue (DWt) dry weight. GoF test: p-value of the Generalized likelihood ratio goodness-of fit test calibrated by wild
 331 bootstrap (B = 10000).

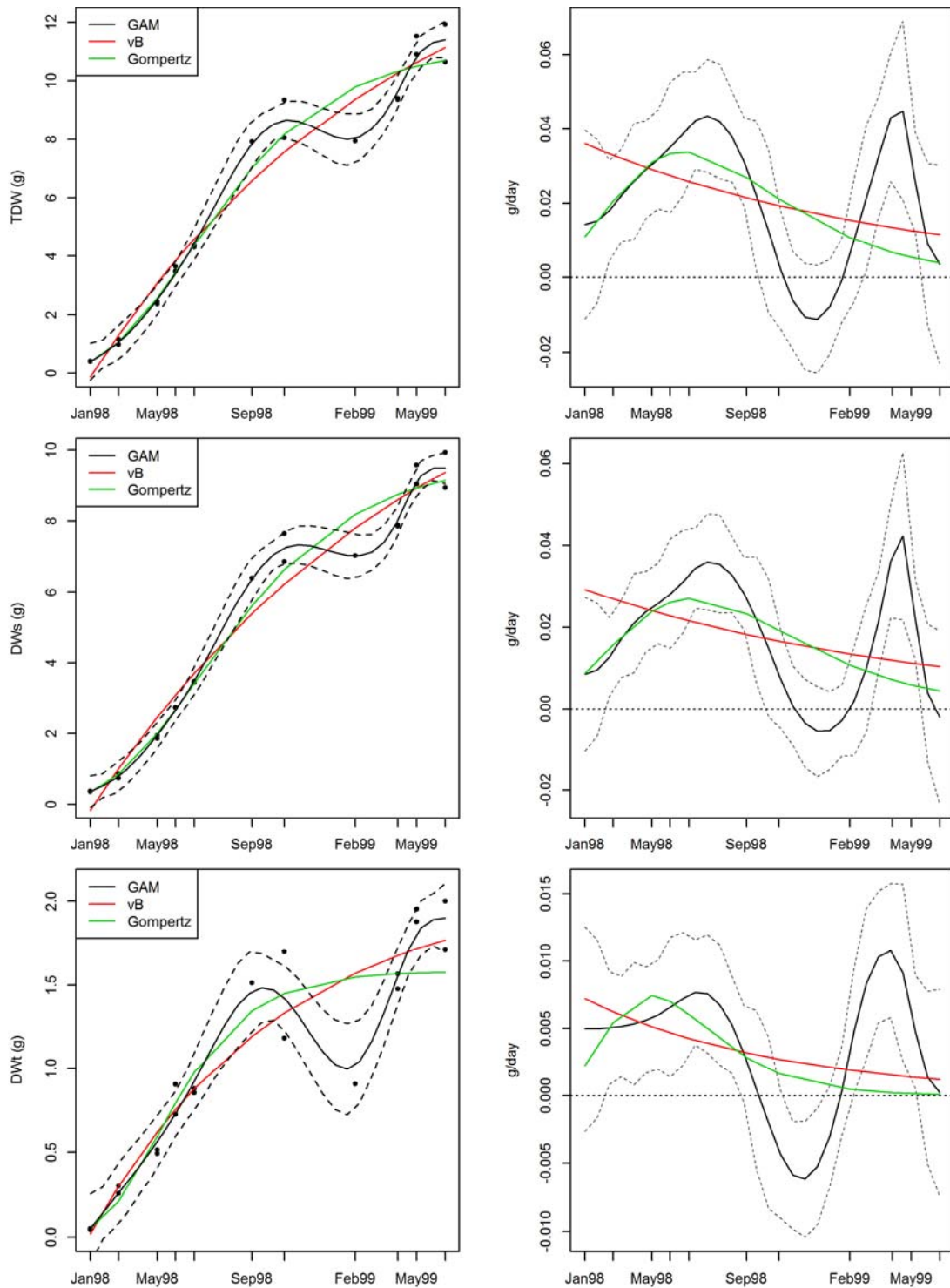
		von Bertalanffy					Gompertz						
		Estimate	Std.Error	t-value	Pr(> t)	GoF test	Estimate	Std.Error	t-value	Pr(> t)	GoF test		
L (mm)	L_{∞}	75.83	1.423	53.28	<2.e-16	***	0.314	72.96	1.043	69.94	<2.e-16	***	0.313
	K	0.175	0.014	12.30	7e-10	***		0.274	0.012	22.18	5e-14	***	
	t_0	-1.760	0.230	-7.661	7e-07	***		0.831	0.077	10.730	5e-09	***	
TDW (g)	w_{∞}	16.44	3.334	4.93	0.0001	***	0.013	11.19	0.469	23.89	2e-14	***	0.065
	K	0.065	0.023	2.87	0.0106	*		0.246	0.012	21.13	1e-13	***	
	t_0	0.163	0.437	0.372	0.7142			4.907	0.242	20.290	2e-13	***	
DWs (g)	w_{∞}	14.57	3.146	4.63	0.0002	***	0.012	9.74	0.423	23.01	3e-14	***	0.056
	K	0.060	0.021	2.83	0.0116	*		0.226	0.011	21.26	1e-13	***	
	t_0	0.232	0.413	0.562	0.5814			5.362	0.266	20.200	2e-13	***	
DWt (g)	w_{∞}	2.118	0.375	5.64	3e-05	***	0.007	1.584	0.122	13.02	3e-10	***	0.01
	K	0.103	0.041	2.48	0.0237	*		0.383	0.038	9.97	2e-08	***	
	t_0	-0.048	0.657	-0.073	0.9426			3.269	0.332	9.858	2e-08	***	

332 (***) p-value < 0.001, (**) p-value < 0.01, (*) p-value < 0.05, (.) p-value < 0.1.

333

334

335



336

337 **Figure B2:** Observed dry weights (points), GAM (black), von Bertalanffy (vB, red) and Gompertz (green) fits of
 338 growth curves (left) and their first derivative (right) for mussels gathered from collector ropes (subtidal mussels).
 339 Fitted values (solid line) and 95% confident intervals (dashed lines) for GAM fit. Top: total dry weight (TDW),
 340 centre: shell dry weight (DWs), bottom: tissue dry weight (DWt).

341

342 **Acknowledgements**

343 We are grateful to Lourdes Nieto and Beatriz Gonzalez for their technical support. We acknowledge Dr.
344 X.A. Álvarez-Salgado for his critical comments that contributed to improve this manuscript. This study
345 was funded by PIE project (CSIC 201540E107), EU H2020 project ClimeFish (EU 677039), and
346 PROINSA-CSIC contract-project (CSIC0704101100001)

347 **References**

- 348 Alonso-Pérez, F., Ysebaert, T., Castro, C., 2010. Effects of suspended mussel culture on benthic–pelagic
349 coupling in a coastal upwelling system (Ría de Vigo, NW Iberian Peninsula). *J. Exp. Mar. Biol.*
350 *Ecol.* 382, 96–107.
- 351 Babarro, J.M., Fernández-Reiriz, M.J., Labarta, U., 2000. Growth of seed mussel (*Mytilus*
352 *galloprovincialis* Lmk): effects of environmental parameters and seed origin. *J. Shellfish Res.*
353 19, 187–193.
- 354 Babarro, J.M., Labarta, U., Fernández-Reiriz, M.J., 2003. Growth patterns in biomass and size structure
355 of *Mytilus galloprovincialis* cultivated in the Ría de Arousa (north-west Spain). *J. Mar. Biol.*
356 *Assoc. UK* 83, 151–158.
- 357 Bagur, M., Richardson, C.A., Gutiérrez, J.L., Arribas, L.P., Doldan, M.S., Palomo, M.G., 2013. Age,
358 growth and mortality in four populations of the boring bivalve *Lithophaga patagonica* from
359 Argentina. *J. Sea Res.* 81, 49–56.
- 360 Bates, D.M., Watts, D.G., 1988. Nonlinear regression: iterative estimation and linear approximations, in:
361 *Nonlinear Regression Analysis and Its Applications*. Wiley, New York, pp. 32–66.
- 362 Bergström, P., Lindegarth, S., Lindegarth, M., 2015. Modeling and predicting the growth of the mussel,
363 *Mytilus edulis*: implications for planning of aquaculture and eutrophication mitigation. *Ecol.*
364 *Evol.* 5, 5920–5933.
- 365 Blicher, M.E., Rysgaard, S., Sejr, M.K., 2010. Seasonal growth variation in *Chlamys islandica* (Bivalvia)
366 from sub-Arctic Greenland is linked to food availability and temperature. *Mar Ecol Prog Ser*
367 407, 71–86.
- 368 Borrero, F.J., Hilbish, T.J., 1988. Temporal variation in shell and soft tissue growth of the mussel
369 *Geukensia demissa*. *Mar. Ecol. Prog. Ser.* Oldendorf 42, 9–15.

370 Brigolin, D., Dal Maschio, G., Rampazzo, F., Giani, M., Pastres, R., 2009. An individual-based
371 population dynamic model for estimating biomass yield and nutrient fluxes through an off-shore
372 mussel (*Mytilus galloprovincialis*) farm. *Estuar. Coast. Shelf Sci.* 82, 365–376.

373 Connor, K.M., Robles, C.D., 2015. Within-Site Variation of Growth Rates and Terminal Sizes in *Mytilus*
374 *californianus* Along Wave Exposure and Tidal Gradients. *Biol. Bull.* 228, 39–51.

375 Cubillo, A.M., Peteiro, L.G., Fernández-Reiriz, M.J., Labarta, U., 2012. Influence of stocking density on
376 growth of mussels (*Mytilus galloprovincialis*) in suspended culture. *Aquaculture* 342–343, 103–
377 111. doi:10.1016/j.aquaculture.2012.02.017

378 Dame, R.F., 1993. The role of bivalve filter feeder material fluxes in estuarine ecosystems, in: *Bivalve*
379 *Filter Feeders*. Springer, pp. 245–269.

380 Díaz, C., Figueroa, Y., Sobenes, C., 2014. Seasonal effects of the seeding on the growth of Chilean
381 mussel (*Mytilus edulis platensis*, d’Orbigny 1846) cultivated in central Chile. *Aquaculture* 428–
382 429, 215–222. doi:10.1016/j.aquaculture.2014.03.013

383 Edwards, M., Richardson, A.J., 2004. Impact of climate change on marine pelagic phenology and trophic
384 mismatch. *Nature* 430, 881–884.

385 Efron, B., Tibshirani, R.J., 1994. *An introduction to the bootstrap*. CRC press, London.

386 Fan, J., Jiang, J., 2007. Nonparametric inference with generalized likelihood ratio tests. *Test* 16, 409–444.

387 Fuentes-Santos, I., Cubillo, A.M., Labarta, U., 2015. A bioeconomic approach to optimize mussel culture
388 production. *Rev. Aquac.* doi:10.1111/raq.12108

389 Gangnery, A., Bacher, C., Buestel, D., 2004. Application of a population dynamics model to the
390 Mediterranean mussel, *Mytilus galloprovincialis*, reared in Thau Lagoon (France). *Aquaculture*
391 229, 289–313.

392 Gompertz, B., 1825. On the nature of the function expressive of the law of human mortality, and on a new
393 mode of determining the value of life contingencies. *Philos. Trans. R. Soc. Lond.* 513–583.

394 Gosling, E., 2003. *Bivalve molluscs: biology, ecology and culture*, Blackwell Publishing. ed. Elsevier,
395 Oxford, UK.

396 Hardle, W., Mammen, E., 1993. Comparing nonparametric versus parametric regression fits. *Ann. Stat.*
397 1926–1947.

398 Hastie, T.J., Tibshirani, R.J., 1990. *Generalized Additive Models*. Chapman and Hall/CRC, London.

399 Hilbish, T.J., 1986. Growth trajectories of shell and soft tissue in bivalves: seasonal variation in *Mytilus*
400 *edulis* L. J. Exp. Mar. Biol. Ecol. 96, 103–113.

401 Irisarri, J., Cubillo, A.M., Fernández-Reiriz, M.J., Labarta, U., 2015. Growth variations within a farm of
402 mussel (*Mytilus galloprovincialis*) held near fish cages: importance for the implementation of
403 integrated aquaculture. Aquac. Res. 46, 1988–2002. doi:10.1111/are.12356

404 Katsanevakis, S., 2007. Growth and mortality rates of the fan mussel *Pinna nobilis* in Lake Vouliagmeni
405 (Korinthiakos Gulf, Greece): a generalized additive modelling approach. Mar. Biol. 152, 1319–
406 1331.

407 Katsanevakis, S., Maravelias, C.D., 2008. Modelling fish growth: multi-model inference as a better
408 alternative to a priori using von Bertalanffy equation. Fish Fish. 9, 178–187.

409 Kautsky, N., 1982. Growth and size structure in a baltic *Mytilus edulis* population. Mar. Biol. 68, 117–
410 133. doi:10.1007/BF00397599

411 Labarta, U., Fernández-Reiriz, P., Pérez-Camacho, A., Alejandro, P., Pérez-Corbacho, E., 2004. Bateeiros, mar,
412 mejillón. Una perspectiva bioeconómica., Serie Estudios Sectoriales. Fundación Caixa Galicia.,
413 A Coruña, Spain.

414 Lewis, D.E., Cerrato, R.M., 1997. Growth uncoupling and the relationship between shell growth and
415 metabolism in the soft shell clam *Mya arenaria*. Mar. Ecol. Prog. Ser. 158, 177–189.

416 Ligas, A., Colloca, F., Lundy, M.G., Mannini, A., Sartor, P., Sbrana, M., Voliani, A., Belcari, P., 2015.
417 Modeling the growth of recruits of European hake (*Merluccius merluccius*) in the northwestern
418 Mediterranean Sea with generalized additive models. Fish. Bull. 113, 69–82.

419 Lindahl, O., Hart, R., Hernroth, B., Kollberg, S., Loo, L.-O., Olrog, L., Rehnstam-Holm, A.-S., Svensson,
420 J., Svensson, S., Syversen, U., 2005. Improving marine water quality by mussel farming: a
421 profitable solution for Swedish society. AMBIO J. Hum. Environ. 34, 131–138.

422 Loo, L.-O., Rosenberg, R., 1983. *Mytilus edulis* culture: Growth and production in western Sweden 35,
423 137–150. doi:10.1016/0044-8486(83)90081-9

424 Lucas, A., Beninger, P.G., 1985. The use of physiological condition indices in marine bivalve
425 aquaculture. Aquaculture 44, 187–200.

426 Mallet, A.L., Carver, C.E.A., Coffen, S.S., Freeman, K.R., 1987. Winter growth of the blue mussel
427 *Mytilus edulis* L.: importance of stock and site. J. Exp. Mar. Biol. Ecol. 108, 217–228.

- 428 Marambio, J., Maturana, S., Campos, B., 2012. Modelo dinámico de crecimiento de la biomasa para
429 *Mytilus chilensis* en sistemas de cultivo en líneas. *Rev. Biol. Mar. Oceanogr.* 47, 51 – 64.
- 430 Marra, G., Wood, S.N., 2011. Practical variable selection for generalized additive models. *Comput. Stat.*
431 *Data Anal.* 55, 2372–2387.
- 432 Martínez-Silva, I., Sestelo, M., Bidegain, G., Lorenzo-Arribas, A., Roca-Pardiñas, J., 2014.
433 Nonparametric regression applied to sea urchin growth, in: *Sea Urchins: Habitat, Embryonic*
434 *Development and Importance in the Environment*. NOVA, Editors: E. Raymond Banks, pp. 1–
435 32.
- 436 Nedoncelle, K., Lartaud, F., De Rafelis, M., Boulila, S., Le Bris, N., 2013. A new method for high-
437 resolution bivalve growth rate studies in hydrothermal environments. *Mar. Biol.* 160, 1427–
438 1439.
- 439 Newell, R.I., Hilbish, T.J., Koehn, R.K., Newell, C.J., 1982. Temporal variation in the reproductive cycle
440 of *Mytilus edulis* L.(*Bivalvia*, *Mytilidae*) from localities on the east coast of the United States.
441 *Biol. Bull.* 162, 299–310.
- 442 Ohnishi, S., Akamine, T., 2006. Extension of von Bertalanffy growth model incorporating growth
443 patterns of soft and hard tissues in bivalve molluscs. *Fish. Sci.* 72, 787–795.
- 444 Okumuş, İ., Stirling, H.P., 1994. Physiological energetics of cultivated mussel (*Mytilus edulis*)
445 populations in two Scottish west coast sea lochs. *Mar. Biol.* 119, 125–131.
- 446 Olsen, E., Knutsen, H., Simonsen, J., Jonsson, B., Knutsen, J., 2006. Seasonal variation in marine growth
447 of sea trout, *Salmo trutta*, in coastal Skagerrak. *Ecol. Freshw. Fish* 15, 446–452.
- 448 Otero, J., Álvarez-Salgado, X.A., González, Á.F., Gilcoto, M., Guerra, Á., others, 2009. High-frequency
449 coastal upwelling events influence *Octopus vulgaris* larval dynamics on the NW Iberian shelf.
450 *Mar. Ecol. Prog. Ser.* 386, 123–132.
- 451 Ozernyuk, N., Zotin, A., 2006. Comparative analysis of growth of edible mussel *Mytilus edulis* from
452 different White Sea regions. *Biol. Bull.* 33, 149–152.
- 453 Pérez-Camacho, A., Aguiar, E., Labarta, U., Vinseiro, V., Fernández-Reiriz, M.J., Álvarez-Salgado, X.A.,
454 2014. Ecosystem-based indicators as a tool for mussel culture management strategies. *Ecol.*
455 *Indic.* 45, 538–548.

456 Pérez-Camacho, A., Labarta, U., Beiras, R., 1995. Growth of mussels (*Mytilus edulis galloprovincialis*)
457 on cultivation rafts: influence of seed source, cultivation site and phytoplankton availability.
458 *Aquaculture* 138, 349–362.

459 Pérez-Camacho, A., Labarta, U., Vinseiro, V., Fernández-Reiriz, M.J., 2013. Mussel production
460 management: Raft culture without thinning-out. *Aquaculture* 406–407, 172–179.
461 doi:10.1016/j.aquaculture.2013.05.019

462 Pernet, F., Malet, N., Pastoureaud, A., Vaquer, A., Quéré, C., Dubroca, L., 2012. Marine diatoms sustain
463 growth of bivalves in a Mediterranean lagoon. *J. Sea Res.* 68, 20–32.

464 Peteiro, L.G., Babarro, J.M., Labarta, U., Fernández-Reiriz, M.J., 2006. Growth of *Mytilus*
465 *galloprovincialis* after the Prestige oil spill. *ICES J. Mar. Sci. J. Cons.* 63, 1005–1013.

466 Peteiro, L.G., Filgueira, R., Labarta, U., Fernández-Reiriz, M.J., 2008. Growth and biochemical responses
467 of the offspring of mussels directly affected by the “Prestige” oil spill. *ICES J. Mar. Sci. J. Cons.*
468 65, 509–513.

469 Peterson, C.H., Fegley, S.R., 1986. Seasonal allocation of resources to growth of shell, soma, and gonads
470 in *Mercenaria mercenaria*. *Biol. Bull.* 171, 597–610.

471 Philippart, C.J., Amaral, A., Asmus, R., van Bleijswijk, J., Bremner, J., Buchholz, F., Cabanellas-
472 Reboredo, M., Catarino, D., Cattrijsse, A., Charles, F., others, 2012. Spatial synchronies in the
473 seasonal occurrence of larvae of oysters (*Crassostrea gigas*) and mussels (*Mytilus*
474 *edulis/galloprovincialis*) in European coastal waters. *Estuar. Coast. Shelf Sci.* 108, 52–63.

475 Rabaoui, L., Zouari, S.T., Katsanevakis, S., Belgacem, W., Hassine, O.K.B., 2011. Differences in
476 absolute and relative growth between two shell forms of *Pinna nobilis* (Mollusca: Bivalvia)
477 along the Tunisian coastline. *J. Sea Res.* 66, 95–103.

478 Rabaoui, L., Zouari, S.T., Katsanevakis, S., Hassine, O.K.B., 2007. Comparison of absolute and relative
479 growth patterns among five *Pinna nobilis* populations along the Tunisian coastline: an
480 information theory approach. *Mar. Biol.* 152, 537–548.

481 Rilov, G., Dudas, S.E., Menge, B.A., Grantham, B.A., Lubchenco, J., Schiel, D.R., 2008. The surf zone: a
482 semi-permeable barrier to onshore recruitment of invertebrate larvae? *J. Exp. Mar. Biol. Ecol.*
483 361, 59–74. doi:10.1016/j.jembe.2008.04.008

484 Rogers-Bennett, L.D., 2003. Modeling red sea urchin growth using six growth functions. *Fish. Bull.* 101,
485 614–626.

486 Sebens, K.P., 1987. The ecology of indeterminate growth in animals. *Annu. Rev. Ecol. Syst.* 371–407.

487 Sestelo, M., Roca-Pardinas, J., 2011. A New Approach to Estimation of the Length—Weight
488 Relationship of *Pollicipes pollicipes* (Gmelin, 1789) on the Atlantic Coast of Galicia (Northwest
489 Spain): Some Aspects of Its Biology and Management. *J. Shellfish Res.* 30, 939–948.

490 Smith, J.M., Pierce, G.J., Zuur, A.F., Boyle, P.R., 2005. Seasonal patterns of investment in reproductive
491 and somatic tissues in the squid *Loligo forbesi*. *Aquat. Living Resour.* 18, 341–351.

492 Snodden, L. m., Roberts, D., 1997. Reproductive Patterns and Tidal Effects on Spat Settlement of *Mytilus*
493 *Edulis* Populations in Dundrum Bay, Northern Ireland 77, 229–243.
494 doi:10.1017/S0025315400033890

495 Suárez, M.P., Alvarez, C., Molist, P., Juan, F.S., 2005. Particular aspects of gonadal cycle and seasonal
496 distribution of gametogenic stages of *mytilus galloprovincialis* cultured in the estuary of vigo 24,
497 531–540. doi:10.2983/0730-8000(2005)24[531:PAOGCA]2.0.CO;2

498 Torres, R., Barton, E.D., Miller, P., Fanjul, E., 2003. Spatial patterns of wind and sea surface temperature
499 in the Galician upwelling region. *J. Geophys. Res. Oceans* 108.

500 Urrutia, M., Ibarrola, I., Iglesias, J., Navarro, E., 1999. Energetics of growth and reproduction in a high-
501 tidal population of the clam *Ruditapes decussatus* from Urdaibai Estuary (Basque Country, N.
502 Spain). *J. Sea Res.* 42, 35–48.

503 von Bertalanffy, L., 1938. A quantitative theory of organic growth (Inquiries on growth laws. II). *Hum.*
504 *Biol.* 10, 181–213.

505 Witbaard, R., Duineveld, G.C., Bergman, M.J., Witte, H.I., Groot, L., Rozemeijer, M.J., 2015. The
506 growth and dynamics of *Ensis directus* in the near-shore Dutch coastal zone of the North Sea. *J.*
507 *Sea Res.* 95, 95–105.

508 Wood, S., 2006. *Generalized additive models: an introduction with R.* Chapman and Hall/CRC, London.

509 Wooster, W.S., Bakun, A., McLain, D.R., 1976. Seasonal upwelling cycle along the eastern boundary of
510 the North Atlantic. *J. Mar. Res.* 34, 131–141.

511 Zúñiga, D., Castro, C.G., Aguiar, E., Labarta, U., Figueiras, F., Fernández-Reiriz, M.J., 2014. Biodeposit
512 contribution to natural sedimentation in a suspended *Mytilus galloprovincialis* Lmk mussel farm
513 in a Galician Ría (NW Iberian Peninsula). *Aquaculture* 432, 311–320.

514

515